# Effect of Thermal History and Microdomain Orientation on Deformation and Fracture Properties of Poly(cyclohexylethylene)−Polyethylene Triblock Copolymers Containing Cylindrical PE Domains

**Janne Ruokolainen, Glenn H. Fredrickson, and Edward J. Kramer***

*Departments of Materials and Chemical Engineering, University of California, Santa Barbara, California 93106*

**Chang Y. Ryu**

*Department of Chemistry, Rensselaer Polytechnic Institute, Troy, New York 12180*

**Stephen F. Hahn**

*Corporate R&D, The Dow Chemical Company, Midland, Michigan 48674*

**Sergei N. Magonov**

*Digital Instruments, Veeco Metrol Grp, Santa Barbara, California 93110*

*Received May 22, 2002*

ABSTRACT: We investigate the effects of polyethylene cylinder domain orientation and thermal history on the micromechanical deformation and fracture properties of poly(cyclohexylethylene)−poly(ethylene)−poly(cyclohexylethylene) (CEC) triblock copolymer where the poly(cyclohexylethylene) (PCHE) blocks are unentangled. The properties are assessed using a "fragility" test in which copolymer films are strained in tension using a copper grid as a support. Optical microscopy was used to determine the statistics of deformation and fracture events while transmission electron microscopy (TEM) and scanning force microscopy (SFM) were used to investigate the morphological details of the plastically deformed regions. Films of CEC show much more ductility if the PE cylinders are oriented either randomly (spun-cast films) or parallel to the tensile direction than if the PE cylinders are perpendicular to the tensile direction. In the latter case craze breakdown and crack propagation can proceed within the unentangled PCHE matrix domain without the highly entangled PE cylinders bridging such cracks. For the highest molecular weight CEC physical aging of the PCHE glassy domains is also important in causing embrittlement. Removing such physical aging by quenching from above the glass transition temperature $T_g$ of PCHE causes a change in deformation mechanism from crazing in slowly cooled samples to a mixed case where crazing and shear deformation compete. Although the crystal morphology in the PE cylinders may also depend on the cooling rate during crystallization, it can be ruled out as the cause of the embrittlement since films physically aged below $T_g$ of PCHE but above the melting temperature of PE show brittle behavior when quenched from the aging temperature.

## Introduction

Excellent optical clarity, low density, and easy processability are properties that make amorphous glassy polymers ideal for many engineering applications. However, often their fracture properties are very poor, leading to premature brittle failure. Polymer ductility can be improved by increasing the molecular weight, but in order to achieve adequate improvements in toughness, a glassy polymer must have a molecular weight of roughly 10 times the entanglement molecular weight $M_e$.[1,2] Unfortunately, processing of such high molecular weight materials is difficult in practice due to their higher viscosity and melt elasticity. Another method to increase polymer fracture toughness is to add rubber particles to the polymer matrix. Rubber particles act as nucleation centers for multiple crazing or shear bands, and a substantial amount of plastic strain can be achieved before material fracture. This method has been successfully used to strengthen a variety of thermoplastic polymers since the 1940s.[3] However, there is a drawback of using rubber-modified polymers in applications requiring high transparency. Small rubber particles are not efficient for nucleating crazes, and the minimum particle diameter typically varies from hundreds of nanometers to a few microns depending on the polymer/modifier system.[4,5] These large particles scatter light strongly unless the refractive index of the matrix and the rubber modifier are precisely matched. However, because of variation of the refractive indices for different wavelengths and temperatures, complete index matching over the whole visible spectrum is very difficult to achieve in practice.[4]

One method of relieving undesirable brittleness of glassy polymers, while retaining an optical clarity and relatively high modulus, is to form block copolymers with glassy and rubbery blocks. These materials are highly transparent because the block copolymers form a variety of different microphase-separated structures via self-assembly with a typical domain size of 5−100 nm.[6,7] If the particle/domain size is small enough (∼0.05 × wavelength of light, i.e., 20−30 nm), the material can be considered optically homogeneous.[5] Early studies showed that polystyrene−polybutadiene (PS−PB) block copolymers having a glassy (PS) matrix can be quite tough. Matsuo et al. found that tetrablock copolymers (SBSB) and triblock copolymers (SBS), where the rubbery PB block was the middle block, were ductile.[8] On

10.1021/ma020791k CCC: $22.00 
Published on Web 11/07/2002

the contrary, triblock copolymers with rubbery end blocks (BSB) and diblock copolymers (SB) were brittle.

Recently, Weidisch et al. have studied the effect of block copolymer morphology and degree of segregation ($\chi N$) on deformation properties of polystyrene-*b*-poly(*n*-butyl methacrylate) (PS−PBMA) block copolymers.[9,10] They found that disordered block copolymers ($\chi N$ < 10.5) with a PS-rich composition had a similar deformation mechanism to that of polystyrene, whereas microphase-separated block copolymers showed improved tensile properties. The greatest improvement in terms of high strength and toughness was observed for intermediately segregated block copolymers ($12.5 < \chi N < 95$). These synergistic effects on the tensile properties for PS−PBMA system were hypothesized to arise from their high miscibility and large interface width. The coexistence of lamellar and hexagonal cylindrical morphologies was also discussed as a possible reason for improved mechanical properties compared to those of pure PS.[9]

Despite this earlier work on deformation and fracture of glassy matrix multiblock copolymers, there has been little attention given to the effects of processing and thermal history on the properties of such block copolymers. Various processing methods (e.g., extrusion) might be expected to produce alignment of domain morphologies that would give rise to anisotropy in the mechanical properties. In addition, the effect of thermal history on physical aging of the glassy matrix and the crystalline morphology within semicrystalline domains may be important.

Physical aging is a structural relaxation process that occurs in a glassy state. If the polymer is aged below its glass transition temperature, the polymer chains relax toward the equilibrium liquid structure. In this process, the polymer specific volume decreases, the shear and Young's moduli increase, and the shear yield stress increases.[11] An effective way to physically age the polymer is to cool it slowly through its glass transition temperature. Although physical aging increases the polymer shear yield stress, it does not increase the crazing stress as strongly, and thus a change in deformation mechanism from crazing to shear deformation may be caused by removing the effects of physical aging by annealing above the $T_g$ and then quenching. A polymer that under normal aging conditions deforms by crazing followed by craze breakdown to form cracks, and subsequent brittle failure may after quenching show ductile deformation by shear yielding. This change of deformation mechanism from crazing to shear yielding has been observed for several glassy polymers.[12] Thermal history also has an effect on crystallization of semicrystalline polymers. If the glass transition temperature of the glassy matrix block is higher than crystallization temperature of the crystalline block, the block copolymer matrix is already vitrified when the crystallization occurs inside the confined domains, and the block copolymer morphology is unaffected by this crystallization process. However, the total degree of crystallinity and PE crystal lamellar thickness may depend on the cooling rate, and changes in these quantities may have an effect on the block copolymer deformation and fracture.

Block copolymer microdomain orientation certainly plays an important role in determining the material deformation properties. For example, the thermoplastic elastomer poly(styrene−butadiene−styrene) (SBS) with a PS cylinder morphology behaves like an elastic rubber if cylinders are oriented perpendicular to the tensile strain but has a typical glassy modulus if the strain is applied parallel to PS cylinders.[13,14] Schwier et al. showed that a blend of PS−PB diblock copolymers with different molecular weights and compositions resulted a very tough material when the morphology was topologically interconnected PB cylinders instead of the straight cylinder morphology typical of pure diblock copolymers.[15] Because of interconnected cylindrical morphology, the polystyrene matrix was able to deform, form stable crazes, and absorb significant amounts of energy before final fracture.

In our previous paper, we investigated the fracture and deformation properties of thin films of poly(cyclohexylethylene)−poly(ethylene) (PCHE−PE) block copolymers.[16] PCHE is a glassy amorphous polymer, which has good optical and thermal properties, excellent clarity, low birefringence, and a relatively high glass transition temperature ($T_g$ = 145 °C). But because of its high entanglement molecular weight ($M_e$ = 49 000 g/mol), PCHE is very brittle even at relatively high molecular weights. We showed that PCHE fracture properties can be considerably improved by using a block copolymer architecture where PE forms cylindrical domains embedded in a glassy PCHE matrix. Triblock copolymers (PCHE−PE−PCHE or CEC) showed a modest increase in craze fibril stability even though the PCHE blocks were so short that they were unentangled. While keeping the total molecular weight and PE weight fraction constant and changing the chain architecture from triblock to pentablock (CECEC), a transition from brittle to ductile behavior was observed.

In this paper we focus on the effects of thermal history and microdomain orientation on the deformation and fracture properties of thin films of CEC triblock copolymers. CEC is a glassy−semicrystalline block copolymer, and depending on the thermal history, the amount of physical aging of the glassy PCHE domains and the crystallization and crystalline morphologies in the semicrystalline PE domains can be different. These aging effects will be seen to have an impact on the polymer fracture properties.

## Experimental Section

**Materials and Thin Film Preparation.** Poly(cyclohexylethylene)−poly(ethylene)−poly(cyclohexylethylene) (PCHE−PE−PCHE or CEC) block copolymers were synthesized by heterogeneous catalytic hydrogenation of polystyrene−polybutadiene (SBS) triblock copolymer precursors. The average 1,2-addition in the PB block was 10% so that after hydrogenation the PE block contains approximately 26 ethyl branches per 1000 backbone carbon atoms. The block copolymer composition was chosen so that the PE blocks form cylinders in a PCHE matrix. The polyethylene block weight fraction was approximately 0.25, and the total molecular weight was varied between 40 000 and 80 000 g/mol. One higher molecular weight sample with a PE weight fraction of 0.29 was also used in some thermal history experiments. The block copolymer compositions, total molecular weights, polydispersity indices, and cylindrical morphology long periods, i.e., spacing of the (10) planes, are presented in Table 1.

The order−disorder transition temperatures (ODT) for each polymer in this study are far above the glass transition temperature of PCHE; thus, all the block copolymers are well segregated before the PCHE matrix vitrifies. Our finding that the ODT for CEC50 is above 300 °C is consistent with other published results[17] where the ODT was determined for a lower molecular weight, but compositionally similar, CEC triblock sample to be 243 °C (total molecular weight of 32 400 g/mol with PE weight fraction of 0.264). The molecular weight

**Table 1. Molecular Weights, Compositions, and Long Periods of PCHE−PE−PCHE Block Copolymers**

| sample | $f_{PE}$ (wt %) | $M_w$ (g/mol) | $M_w/M_n$ | spacing of (10) planes[a] (nm) |
|---|---|---|---|---|
| CEC40 | 0.25 | 40 000 | 1.02 | 17.9 |
| CEC50 | 0.24 | 50 130 | 1.02 | 20.8 |
| CEC61 | 0.25 | 61 100 | 1.02 | 24.0 |
| CEC72 | 0.23 | 72 410 | 1.09 | 26.2 |
| CEC80 | 0.24 | 80 560 | 1.1 | 30.3 |
| CEC107 | 0.29 | 107 000 | 1.04 | 38.5 |

[a] Determined for annealed and slowly cooled bulk block copolymer samples using SAXS.

dependence of the long period is characteristic for the intermediate segregated block copolymers with the scaling $L_p \sim M_w^{0.8}$, where $M_w$ is the block copolymer total molecular weight.

Uniform thin films of block copolymer were spun-cast from hot decahydronaphthalene solutions on hot sodium chloride (NaCl) crystal substrates at 2000 rpm. The temperature of the NaCl substrate was approximately 120 °C and was controlled by using an IR lamp. The film thickness was about 0.7 $\mu$m as measured by using a Dektak II profilometer. Part of the samples was annealed on NaCl crystals at 190 °C for 3 days under high vacuum ($<10^{-6}$ mbar) followed by either slow cooling (0.5 °C/min) or fast quenching. The advantage of using sodium chloride crystal substrates (Aldrich, FTIR windows, 2 mm thick and 25 mm diameter) is that, besides the fact that their surfaces are quite smooth, annealed films can be easily floated off them onto the water surface. This is not the case for other smooth substrates such as Si.

**Fragility Testing: Copper Grid Experiment.** The micromechanical deformation behavior was investigated by using a so-called fragility test[1,18] where the thin polymer films are tested in tension using copper grids as a support. The bare copper grids were first annealed at 600 °C under vacuum for 10 min to recrystallize the copper. The spin-cast or annealed polymer films were floated off NaCl crystals onto the surface of a water bath and picked up on these ductile copper grids. Prior to film pick-up, the grid bars were dip-coated with a thin layer of homopolymer (PCHE). To ensure that the polymer film bonds securely to grid bars, the films on the grids were exposed for a short time to warm toluene vapor. Such exposure simultaneously relaxes some of the biaxial orientation in the film and causes the film to shrink in area and pull taut over each grid square. The film shrinkage was more pronounced for samples that were directly floated to the grids after spun-casting without any annealing procedures. Traces of toluene, which may act as an environmental crazing agent, were removed by drying the bonded film squares under the vacuum at room temperature. The copper grids are subsequently deformed at room temperature in tension at a slow strain rate ($1 \times 10^{-4}$ s$^{-1}$). The steady slow deformation rate was achieved by using translation stage equipped with a motor and gear head. Depending on the film size, each copper grid contains 20−50 individual polymer film squares. During the slow tensile test information about craze initiation, craze breakdown and fracture can be obtained by inspecting the film squares at various strains under an optical microscope using reflected light. A craze or a crack in a one film square does not propagate to adjacent film squares, thus making statistical analysis possible. Each fragility test result shown in this paper consists of an average of at least three different copper grids, i.e., an average of 60−150 individual film squares.

**Large-Amplitude Oscillatory Shear.** Solid rectangular-shaped samples of neat block copolymer were prepared by compression-molding of polymer pellets at 210 °C. The sample was oriented by using reciprocating shear at 215 °C for 2 h followed by slow cooling to room temperature. A sample thickness of 1 mm was maintained during the shear. The maximum shear displacement was ±5 mm, which gives a strain amplitude of 500%. The strain rate was approximately 0.4 s$^{-1}$. Shear oriented samples were microtomed at room temperature using a diamond knife to produce films of 1.0 $\mu$m in thickness and area of 5 mm × 5 mm for fragility testing.

**Small-Angle X-ray Scattering.** Copper Kα radiation ($\lambda$ = 1.54 Å) was generated by a Rigaku rotating anode generator and monochromated by an Osmic confocal Maxflux double-focusing multilayer mirror. Two-dimensional diffraction data were collected with a Bruker HI-STAR detector, and the sample-to-detector distance was 1.515 m. The SAXS intensity patterns were collected at ambient temperature.

**Transmission Electron Microscopy (TEM) and Scanning Force Microscopy (SFM).** TEM images were recorded at 200 kV with a JEOL 2000FX instrument. After the fragility test, a typical film square was carefully cut from the copper grid with a razor blade and examined by TEM. The plastically deformed copper grid holds the polymer film under tension during TEM imaging. All samples were analyzed within few hours after deformation.

The morphological characterization of shear-oriented samples was done by using a sample preparation technique that relies on different rates of diffusion of the $RuO_4$ stain into the amorphous and semicrystalline regions.[19,20] First, the sample surface was cut at room temperature to make a smooth surface for the stain to penetrate into the sample. In our case microtoming at ambient temperatures was possible because majority of the sample consists of glassy PCHE. The sample was then immersed into a 0.5% $RuO_4$-stabilized aqueous solution (Electron Microscopy Science) for 5−7 days. The stained sample was microtomed using a Leica Ultracut UCT ultramicrotome with a diamond knife at room temperature, and 80 nm thick sections were collected on 600 mesh hexagonal grids. For cross-sectional TEM the film was stained in $RuO_4$ vapor for 10 h. During the staining the film was still on a NaCl substrate. The film was then floated off onto the water surface and embedded in epoxy. Cross sections were microtomed at room temperature using diamond knife.

Low-angle electron diffraction (LAED) patterns were recorded using a high-dispersion diffraction mode. The objective aperture was used to select the area from which the electron diffraction patterns were recorded. The camera length was calibrated to be 82.7 m using a carbon waffle grating with 463 nm line spacing.

Scanning force microscopy (SFM) studies of the PCHE−PE block copolymers were performed with a scanning probe microscope MultiMode Nanoscope IIIA (Digital Instruments/Veeco Metrology Group). All measurements were conducted at ambient conditions in tapping mode with etched Si probes (stiffness 1−3 N/m). Height and phase images were recorded simultaneously. The driving frequency was adjusted to the resonant frequency of the probe in immediate vicinity of a sample surface. The initial amplitude of the probe oscillation and the set-point amplitude applied for imaging were chosen to maximize the image contrast differentiating the PCHE and PE domains.

**Differential Scanning Calorimetry (DSC).** Thermal analysis measurements were performed using TA Instruments 2920 calorimeter. Before the DSC measurements block copolymer samples were annealed in aluminum DSC pans for 3 days at 190 °C under high vacuum ($<10^{-6}$ mbar). One sample was allowed to slowly cool back to room temperature at the rate of about 0.1 °C/min, whereas another sample was rapidly cooled by quenching it in a water bath. The DSC measurements were recorded during the first heating scan with the rate of 10 °C/min.

## Results and Discussion

**Block Copolymer Morphology and Microdomain Orientation.** To find out how the block copolymer microstructure evolves during the annealing process, SFM images were taken before and after annealing. SFM imaging was done using the same 0.7 $\mu$m thick films that were used later in the fragility test. During the SFM analysis polymer films were still on the NaCl substrates. The contrast in the tapping mode SFM images is due to mechanical contrast between the glassy PCHE matrix and the softer PE cylinders. Under light

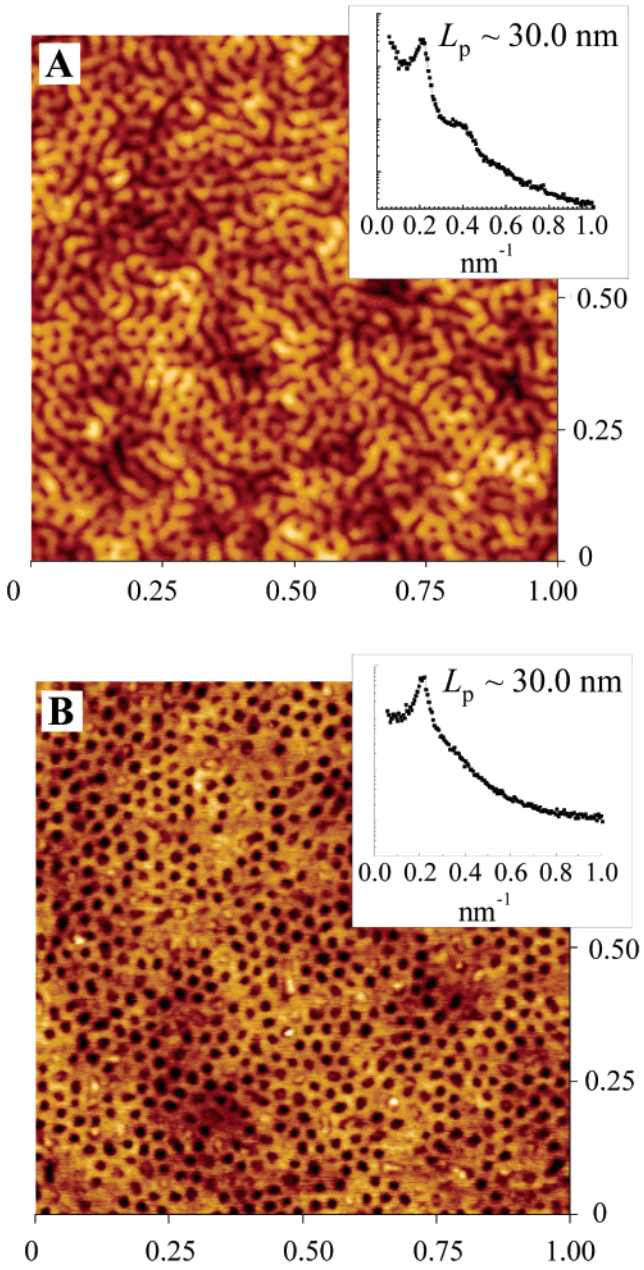


**Figure 1.** Tapping mode SFM image of the CEC80 block copolymer film, 1 $\mu$m scan: (A) as spin-cast sample and (B) annealed sample. PE domains appear darker, because the SFM tip penetrates further into the softer PE domains. Block copolymer morphology is clearly cylindrical and cylinder orientation is random in spin-cast samples, but after annealing the PE cylinders orient normal to the film plane. The FFT power spectra are shown in the insets. The height scale is 8 nm in image a and 6 nm in image b.

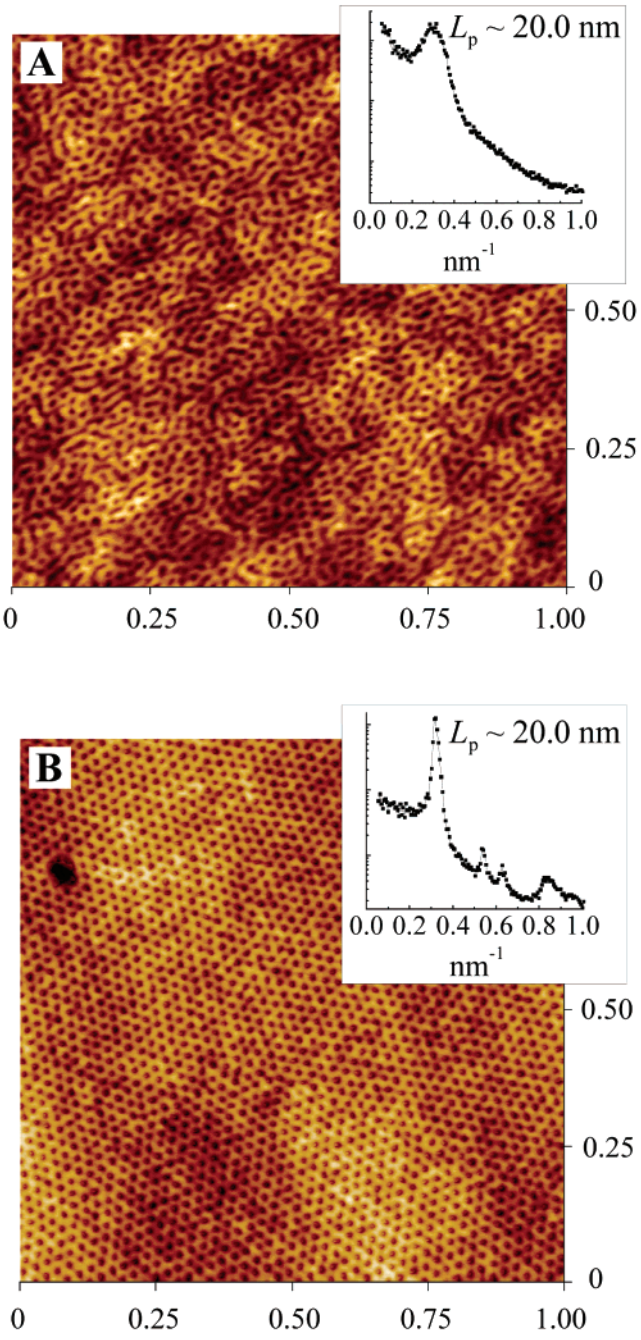


**Figure 2.** Tapping mode SFM image of a CEC50 block copolymer film, 1 $\mu$m scan: (A) as spun-cast sample and (B) annealed sample. The FFT power spectra are shown in the insets. The height scale is 8 nm in both images.

tapping conditions height contrast is negligible, and moderate tapping force is required to achieve contrast between PCHE and PE domains. Figure 1A shows a SFM image taken directly after spin-casting of the CEC80 polymer. The FFT power spectrum is shown in the inset of the upper right corner. The block copolymer morphology is clearly cylindrical, with the PE cylinders being embedded in a PCHE matrix. The cylinder lateral organization shows only very short-range order. Spun-cast polymer films were annealed on NaCl substrates for 3 days in a high vacuum ($<10^{-6}$ mbar) oven at 190 °C followed by slow cooling back to room temperature at about 0.5 °C/min. After annealing, the PE cylinders are clearly oriented normal to the film surface as seen from Figure 1B. The lateral order of the cylinders is still quite poor, although one can observe some regions where the cylinders are packed in a hexagonal lattice.

The ordering is more pronounced for lower molecular weight samples. For example, the CEC50 polymer with a total molecular weight of 50 000 g/mol has orientation kinetics so fast that cylinders tend to orient normal to surface even directly after spin-casting (Figure 2A). However, cylinders are not yet ordered laterally in any particular lattice. Also, the FFT power spectrum shows only one broad peak. After annealing at 190 °C cylinders form highly ordered domains where they are packed in a hexagonal lattice (Figure 2B). In this case the FFT

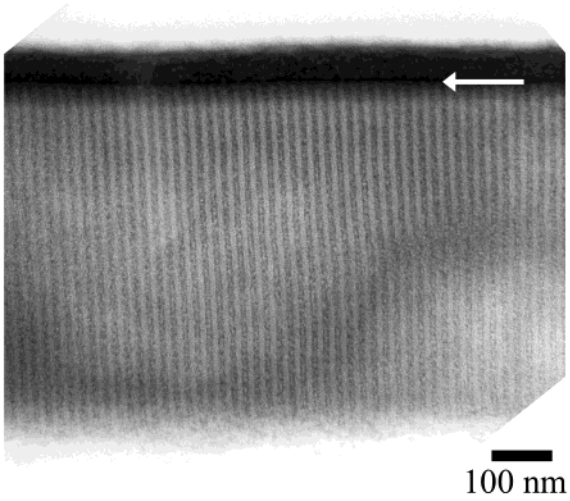


**Figure 3.** Cross-sectional transmission electron micrograph of the annealed CEC50 film. After annealing the film was stained in $RuO_4$ vapor, embedded in epoxy, and cross-sectioned. The $RuO_4$ penetrates most easily into the amorphous PE regions, and therefore the PE cylinders appear dark in the image. The crystalline PE in the cylinder core is least stained and almost white. The PE cylinders are clearly oriented perpendicular to the film surface. Note that the dark 50 nm thick layer on the top surface is due to contamination from $RuO_4$ staining, and the real film surface is marked by the white arrow.

power spectrum shows sharp peaks at the position ratios of $1:\sqrt{3}:2:\sqrt{7}$, which is typical for hexagonal cylinder packing.

Figure 3 shows a cross-sectional TEM image from an annealed CEC50 film. It is clearly evident that PE cylinders are oriented perpendicular to the film surface throughout the bulk of the film. It is very unusual for cylindrical domain block copolymer systems to orient the cylinders normal to a relatively thick film surface as an equilibrium structure. Typically, the polymer block with the lower surface energy forms a thin polymer brush layer at the surface, which influences the block copolymer domain orientation inside the film. Block copolymers with a lamellar or cylindrical morphology have a tendency to form structures where microdomains are oriented parallel to film interfaces. Only when the polymer surface energies are closely matched is a perpendicular orientation observed.[21,22] We believe that the nearly equal surface energies of PE and PCHE are responsible of this unusual cylinder orientation in CEC block copolymer films. When we modify the PE block surface energy by increasing the 1,2 PB content of the precursor from 10% to 40%, maintaining the same PE volume fraction, we observe cylinders laying parallel to the film surface. These additional surface-active methyl groups lower the PE domain surface energy, and the PE chains form a brush layer to the surface. The fact that the PE block is a short midblock also produces an entropy penalty to placing a PE brush layer at the surface, but this can evidently be compensated by increasing the concentration of ethyl branches.

**Deformation Mechanism: As Spin-Cast Films vs Annealed Films.** The deformation and fracture properties of the polymer films are investigated using the fragility test, which allows one to determine the onset of crazing/shear deformation and fracture in each film square as a function of strain by using optical microscopy. In these films crazing is always observed prior to

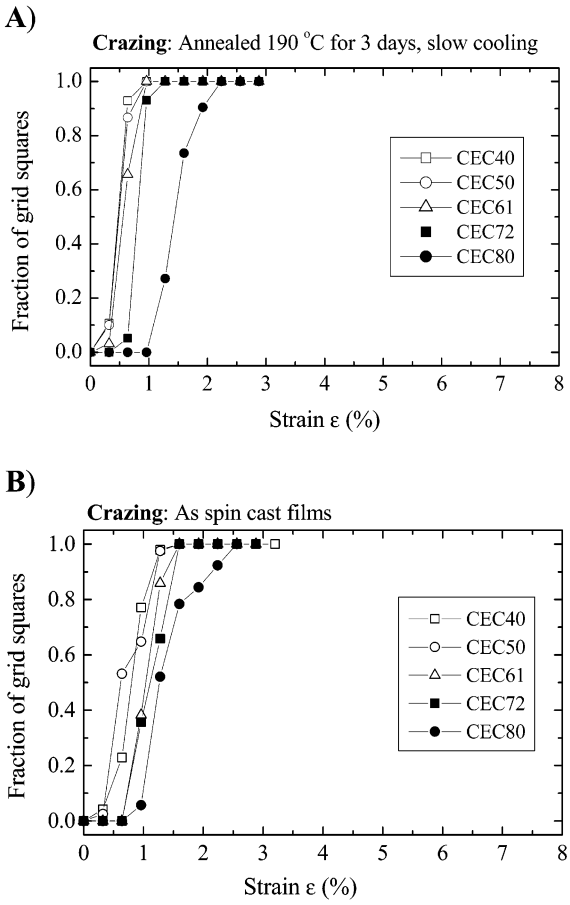


**Figure 4.** Cumulative number fraction of block copolymer film squares that have crazed as a function of strain: (A) prior to the test, the block copolymer film was annealed on NaCl substrates at 190 °C for 3 days and slowly cooled back to the room temperature; (B) as spin-cast films.

fracture regardless of thermal history or molecular weight. This result is similar to what is observed for homopolymer glassy films where cracks are observed to initiate within crazes due to the breakdown of craze fibril structure in the active zone where polymer is being drawn into the craze.[1,18] The cumulative fraction of the film squares in which crazing has occurred is shown in Figure 4A for annealed samples and in Figure 4B for spun-cast samples. The onset for crazing does not depend significantly on the different thermal history of the samples. In both cases the onset for crazing occurs between 0.3% and 1.0% strain depending on the molecular weight of the block copolymers.

**Craze Microstructure.** The block copolymer molecular weight and the thermal history have a strong influence on the craze microstructure. Qualitatively, the craze morphology of the CEC block copolymers is very similar to that of many glassy homopolymers—the craze consists of small main fibrils that are interconnected by short cross-tie fibrils embedded in a continuous void space. However, the main fibril spacing and the cross-tie fibril spacing strongly depend on the block copolymer molecular weight and the thermal history.

Low-angle electron diffraction (LAED) can be used to obtain detailed information on the craze microstructure.[23,24] Figure 5A shows a low-magnification TEM image taken from the spun-cast CEC107 sample at the strain of 11.5%. The selected area, where the diffraction pattern shown in Figure 5B is obtained, is marked on the image with a white circle. Because of the difficulty

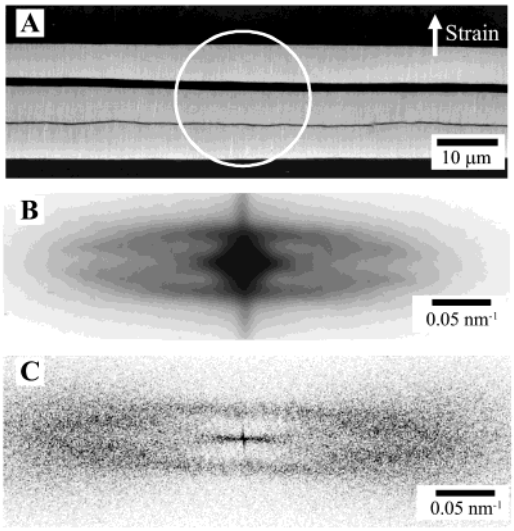


**Figure 5.** (A) Low-magnification TEM image showing the selected area from which the low-angle diffraction pattern (LAED) was obtained. As spin-cast CEC107 block copolymer at the strain of 11.5%. (B) The LAED pattern from the craze area shown in (A). (C) The FFT spectrum from the TEM micrograph, as spin-cast CEC107 at the strain of 11.5%.

of growing wide enough crazes to fill entirely the smallest available aperture size (22 $\mu$m), the area encloses three separate crazes. The LAED pattern shows a strong diffraction both parallel and perpendicular to the craze interfaces. The diffraction streaks parallel to the craze interface are due to scattering from the craze main fibrils. Note that these streaks are split into the two streaks, which are separated by about 12°, showing that the craze main fibril direction is misaligned with respect to the tensile axis by ±6°. The strongly elongated diffraction spots in the direction perpendicular to the craze interface are due to the weakly periodic arrangements of voids. The average distance between the cross-tie fibrils can be determined from the position of the intensity maximum. Additional narrow intensity streaks perpendicular to the craze interface are an artifact due to the reflected or refracted electron beams from the craze−bulk polymer film interfaces.[24,25]

Similar information about the craze microstructure can also be obtained from the TEM micrographs by taking the FFT spectra. Figure 5C shows the TEM micrograph FFT spectrum from the same sample that was used to obtain the LAED patterns. The appearance of the FFT spectrum is very similar to that of the LAED pattern, and the values for the cross-tie fibril spacing and the main fibril spacing determined from the FFT spectrum are identical to those determined from the LAED pattern. We used mainly the FFT spectra to analyze the craze microstructures due to the difficulty of growing wide enough crazes for the LAED. The main fibril spacing is approximately 40 nm for the spun-cast CEC50 sample, and it increases up to 60−70 nm for the spun-cast CEC107 sample. The corresponding values for the cross-tie fibril spacings are 115 nm for the CEC50 sample and 260 nm for the CEC107 sample.

Transmission electron microscopy images also reveal some differences in the craze microstructure due to the different sample thermal history. Parts A and B of Figure 6 show the TEM images of the craze structures for the annealed and the spin-cast CEC80 samples, respectively. The annealed sample shows coarser-meshed net of voids; i.e., the distance between the cross-tie fibrils is larger. The values for the cross-tie fibril spacings, as determined from the TEM image FFT spectra, are 220 nm for the spin-cast film and approximately 280 nm for the annealed film.

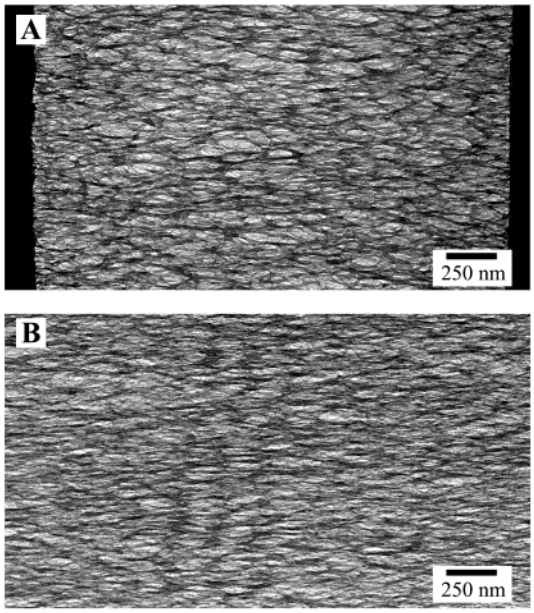


**Figure 6.** Transmission electron micrographs showing the craze microstructure in the CEC80 films having different thermal histories: (A) annealed 3 days at 190 °C followed by slow cooling at the strain of 3%; (B) as spin-cast sample at the strain of 20%.

**Fracture: As Spin-Cast Films vs Annealed Films.** Figure 7A shows the cumulative fraction of film squares where a crack has initiated and propagated over at least half of the film square length for annealed samples. The lowest molecular weight samples show little if any stable craze growth. A crack initiates and grows to fracture the film square immediately after crazing. Higher molecular weight samples also fail soon after crazing if they have been annealed and slowly cooled back to room temperature. The median strain for failure increases slightly with the molecular weight, and the value of 2.9% determined for CEC80 sample is in good agreement with our previously reported value of 3.3% for a slightly higher molecular weight CEC107 sample.[16]

Figure 7B shows the cumulative fraction of grid squares where the film has failed for nonannealed samples. The lowest molecular weight samples are still very brittle, and film squares fail soon after craze initiation. However, the higher molecular weight samples CEC72 and CEC80 do not show any failure before the copper grid fails at strains of about 25%. These results show that, depending on the thermal history, the same polymer film can be either very brittle and fail at low strains or it can show considerable ductility up to large strains.

What are the reasons for this "ductile"[26] to brittle transition? One obvious difference between the annealed and nonannealed samples is found in their block copolymer microstructure. After annealing, PE cylinders are oriented normal to the film surface, whereas the cylinder orientation is more random directly after spin-casting. When cylinders are oriented normal to the film surface, they are also perpendicular to the strain, which can make the crack propagation much easier. But note that due to the different sample thermal histories, there

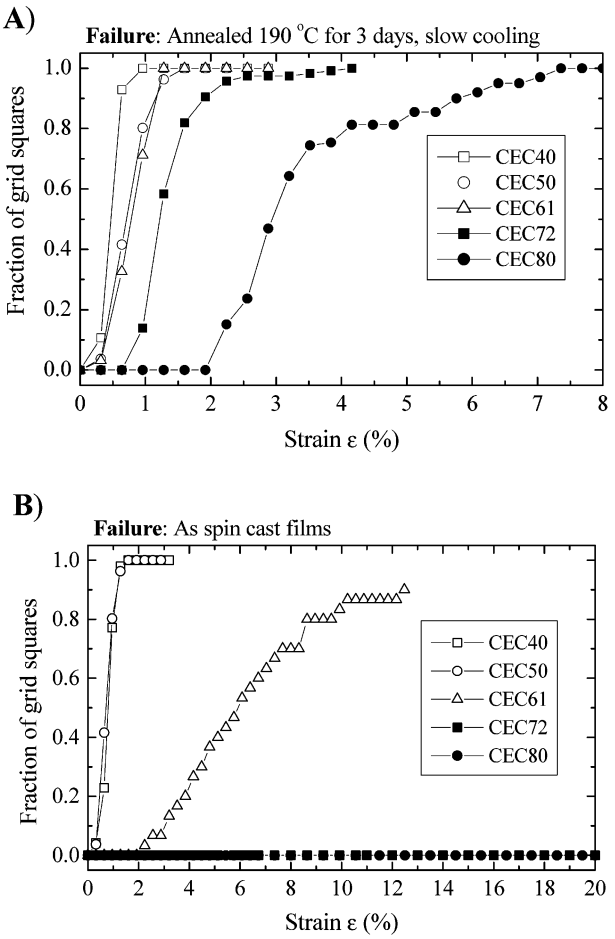


**Figure 7.** Cumulative number fraction of block copolymer film squares that have failed as a function of strain: (A) annealed at 190 °C for 3 days and slowly cooled back to the room temperature and (B) as spin-cast films.

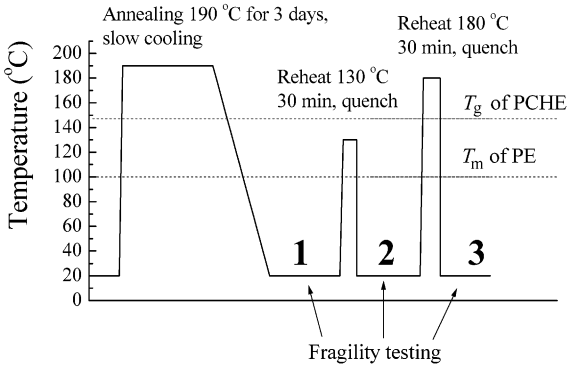


**Figure 8.** Sample thermal history profiles that were used to obtain the fragility test results shown in Figure 9: sample 1 annealed at 190 °C for 3 days followed by slow cooling (0.1 °C/min) back to the room temperature (RT); sample 2 annealed at 190 °C for 3 days and slowly cooled back to RT then reheated to 130 °C for 30 min and fast quenched to RT; sample 3 annealed at 190 °C for 3 days and slowly cooled back to RT, then reheated to 180 °C for 30 min, and fast quenched to RT.

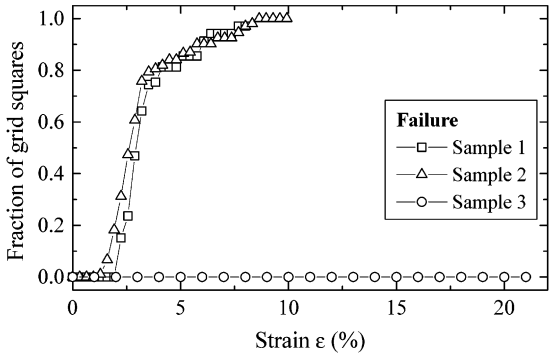


**Figure 9.** Cumulative number fraction of film squares that have failed as a function of strain for CEC80 block copolymer films having different thermal histories. The thermal history profiles are shown in Figure 8.

are also other mechanisms that may have a significant effect on the polymer fracture properties. The annealed samples were slowly cooled through the $T_g$ of PCHE, and thus they have been physically aged more than the spun-cast samples. Also, the PE crystallinity may be different due to this slow cooling process. In the spin-casting process the solvent is evaporated quickly at 120 °C, and thereafter the polymer film is rapidly cooled back to room temperature.

To determine whether cylinder orientation/ordering or physical aging/crystallization are responsible for this ductile-to-brittle transition, the following experiment was performed: After spin-casting, the CEC80 sample was heated to 190 °C only for short period (10 min) and then slowly cooled back to RT (0.5 °C/min). This short annealing time is not long enough to cause any significant changes in long-range domain ordering. We can now compare deformation of this sample to the sample that underwent both annealing for a longer period (3 days) and slow cooling. Because of the same cooling rates, both samples have the same amount of physical aging of the PCHE and identical crystallization conditions for the PE. Fragility test results show that the CEC80 sample is still ductile after the 10 min annealing at 190 °C and slow recooling to RT, which indicates that random orientation of the cylindrical morphology is very beneficial for improving block copolymer fracture properties. However, we note in addition that physical aging plays a significant role in determining the deformation and fracture properties of CEC polymers, as will be shown in the next sections.

**Effect of Thermal History: PCHE Physical Aging vs PE Crystallization.** We noticed that even annealed samples, where the cylinders are oriented normal to film surface and therefore perpendicular to the tensile strain in the fragility test, can be ductile. If after annealing the polymer film (CEC80) for 3 days at 190 °C it is quenched quickly back to room temperature, the sample does not show failure in the fragility test, whereas annealed but slowly cooled samples are brittle. In this case the only differences between the slowly cooled sample and the quenched sample are the amount of physical aging of the PCHE and the different crystallization conditions of the PE. To find out whether PCHE physical aging or PE crystallization was responsible for this ductile-to-brittle transition, the thermal history profiles shown in Figure 8 were used.

A spun-cast CEC80 polymer film was annealed at 190 °C for 3 days followed by a slow cooling back to room temperature. The annealed polymer film was cut into smaller pieces and floated onto the water surface. Films were picked up on copper grids, and the first sample was tested at this point (Figure 9, sample 1). The sample is brittle since due to its slow cooling rate, it has a lot of time for both PCHE physical aging and PE crystallization. A new sample, from this same annealed polymer film, was reheated to 130 °C for 30 min and quickly quenched back to room temperature using a

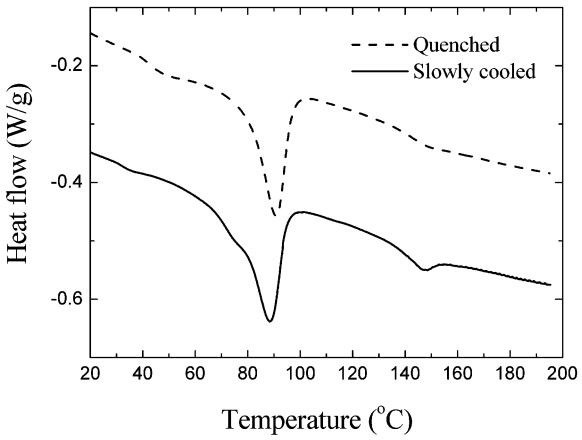


**Figure 10.** DSC scans for the CEC80 samples recorded during the first heating cycle. Prior to the DSC measurements, samples were annealed at 190 °C for 3 days followed by either slow cooling or fast quenching back to the room temperature.

water bath. The 130 °C temperature is above the melting point of PE (melting range approximately 80−100 °C as measured by DSC) but below the glass transition temperature of PCHE ($T_g$ = 145 °C). After drying the traces of water in a vacuum oven at RT, this sample was tested in a fragility test (Figure 9, sample 2). It is still brittle, and its behavior is almost identical with the sample 1. Both samples have now approximately same amount of physical aging (reheat temperature was well below the $T_g$ of PCHE) but quite different cooling conditions for PE crystallization. Sample 1 is slowly cooled through melting point of PE whereas sample 2 is rapidly quenched. The similarity of the results demonstrates that these different PE crystallization conditions do not have significant effects on ductile-to-brittle transition of CEC block copolymers.

To finally prove that physical aging is responsible for this ductile-to-brittle transition observed for CEC block copolymers, the annealed and slowly cooled polymer film was reheated to 180 °C for 30 min and quenched back to room temperature using a water bath (sample 3). Now the crystallization conditions for PE are identical with those of sample 2 (both are fast quenched), but sample 3 has much less physical aging (fast quenching through the $T_g$ of PCHE). Sample 3 is ductile and does not show any failure up to the 20% strain tested.

The effect of cooling rate on the crystallinity of the PE domains was also studied using DSC measurements. CEC80 block copolymer samples were first annealed in aluminum DSC pans for 3 days at 190 °C followed by different cooling procedures. One sample was allowed to slowly cool back to RT at a rate of about 0.1 °C/min, whereas another sample was rapidly cooled by quenching it in a water bath. The DSC measurements are shown in Figure 10, and they were recorded during the first heating scan. The high-temperature parts of the endothermic melting peaks are very similar for both samples and thus are not affected by the cooling rate. The only minor differences are in the region (35−80 °C) of the low-temperature endothermic hump that corresponds to the melting of the small PE crystals.[27] A large abundance of these small PE crystals is quite natural, because the melting temperature of PE is lower than the glass transition temperature of PCHE so the crystallization of PE takes place in the confined nanosized cylindrical domains. This broad low-temperature tail in the melting peak makes the baseline definition for heat of fusion ($H_m$) integration inadequate. When integrating the peak areas, we extended the high-temperature baseline to its intercept with the heating trace at low temperatures.[17,27] The crystallinity was calculated using the measured $H_m$, the PE weight fraction $w_{PE}$ = 0.24, and the theoretical value of heat of fusion 277 J/g[28] for 100% crystalline linear PE. Values of crystallinity were 29.9% and 29.4% for slowly cooled and quenched samples, respectively. The total degree of crystallinity is almost equal in both cases and agrees well with the values Bates and co-workers found for a CEC triblock copolymer with similar molecular weight and composition having thermal history of 20 °C/min cooling from melt.[17] Although the cooling rate seems to have very little influence on the total degree of crystallinity, the PE crystallite size distribution and crystal lamellae thickness may be quite dissimilar. However, in the case of the CEC system, these different PE crystallization conditions seem to make only minor contributions to the deformation and fracture properties compared with the effects of physical aging of the PCHE domains.

It is also evident from the DSC curves that the slowly cooled sample has a considerable amount physical aging. The slowly cooled sample has an endothermic peak at the glass transition temperature, whereas the quenched sample shows only a change in the slope, which is a more typical behavior for glassy amorphous polymers at $T_g$. For physically aged amorphous polymers the enthalpy overshoot around the glass transition temperature is observed to develop simultaneously with the increase in the yield stress.[29] Although physical aging is known to raise the shear yield stress, it has little effect on the crazing stress. If the polymer shear yield stress is higher than the crazing stress, deformation by crazing is expected to dominate. Slowly cooled and therefore physically aged CEC block copolymers were very brittle, and the deformation mechanism was crazing. Even the highest molecular weight samples tested showed brittle fracture at low strains. However, when the effect of physical aging was removed by quenching from above the $T_g$ of PCHE, the CEC80 sample did not show any failure at the fragility test. Nevertheless, for this polymer with a molecular weight of 80 000 the main deformation mechanism was still crazing. The shear deformation mechanism becomes dominant when the molecular weight is increased further. This effect was studied by using the triblock copolymer CEC107, which has a molecular weight of 107 000 g/mol and a PE weight fraction of 0.29. This polymer shows brittle fracture at a median strain of 3.3% if annealed and physically aged by slowly cooling from the melt.[16] The quenched sample does not show any failure in a fragility test, and the deformation mechanism is now mixed, where crazing and shear deformation zones are present at the same sample. Crazing appeared first, but shear deformation becomes dominant when the crazes grow wider. This kind of behavior is expected because the first crazes appear near dust particles and other stress concentration sites, and their craze interface velocity is high. This locally higher strain rate increases the shear yield stress more than it does the crazing stress. Later, however, as crazes grow larger and more crazes nucleate, the interface velocity is lower and shear deformation zones may be favored.[18] Similar mixed deformation mechanisms, where crazing is observed first, are also found in cross-linked PS samples. In this case the crazing stress is increased by the cross-linking,

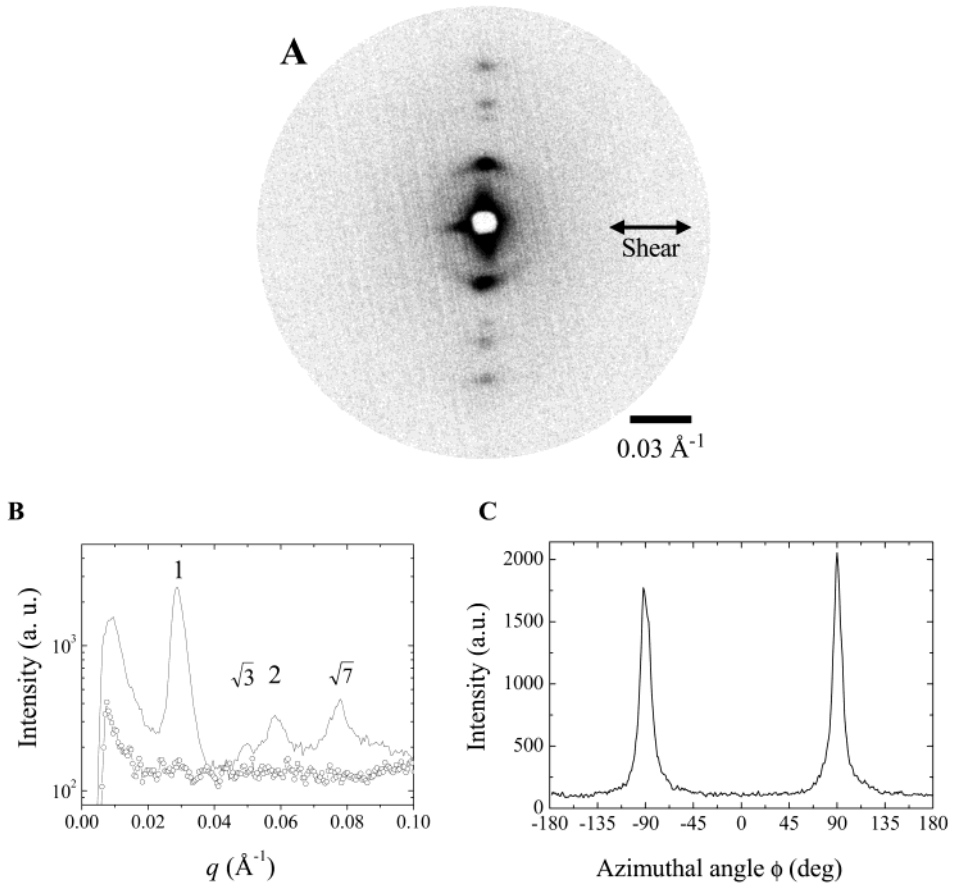


**Figure 11.** (A) Small-angle X-ray diffraction pattern from 1 mm thick bulk CEC50 block copolymer sample oriented by the large-amplitude oscillatory shear. (B) The 20° sector integrations of intensity along the 0° direction (open circles) and along the 90° direction (solid line), where angles are measured relative to the shear direction. (C) The integrated intensity of (10) reflection vs azimuthal angle ($I_{10}(\phi)$ vs $\phi$).

but the shear yield stress is not affected. Increasing the cross-linking density causes the crazing stress to become higher than the shear yield stress, and the deformation mechanism is changed from crazing to shear deformation. This transition is not abrupt, and there is a range of cross-linking densities where both mechanisms are present in the same sample.[18,30]

**Large-Amplitude Oscillatory Shear.** In previous sections it was shown that PE cylinder orientation has a strong influence on the deformation characteristics of these materials. Annealed and slowly cooled films, which have PE cylinders oriented normal to the film surface and thus perpendicular to the strain direction in the tensile test, are very brittle. In contrast, films, with identical cooling rates but annealed for only a very short time at 190 °C, resulting in retention of a more random cylinder orientation, are ductile. To study the effect of cylinder orientation on the deformation and fracture properties in more detail, a large-amplitude oscillatory shear apparatus was used to macroscopically orient cylindrical PE microdomains in the PCHE matrix.

Shear flow application is a very efficient way to align domains in bulk samples of block copolymers.[31] In the case of triblock copolymers with cylindrical morphology the parallel orientation is commonly observed where the cylinder axes are oriented parallel to shear flow. In our study all shear experiments were performed using the rather low molecular weight sample CEC50. To make this sample as brittle as possible after shear, the sample was slowly cooled back to room temperature. Without shear orientation this polymer was very brittle in a fragility test regardless of the sample thermal history.

Figure 11A shows SAXS pattern recorded at room temperature after the shear. The shear direction is marked in Figure 11A by the arrow. Diffraction spots along a (90°) normal to the shear direction in a two-dimensional SAXS pattern were observed and are consistent with the cylinders being oriented along the shear direction. Because the cylinders axes are oriented parallel to the film surface and thus normal to the incident X-ray beam, we do not obtain the typical six spot hexagonal symmetry in a two-dimensional diffraction pattern. One can clearly see the first four reflections (10), (11), (20), and (21) at the diffraction vector magnitude ratios given by $1:\sqrt{3}:2:\sqrt{7}$. The position of the first-order peak at 0.029 Å$^{-1}$ corresponds to 21.6 nm lattice spacing.

Figure 11B shows a 20° sector integration of intensity along 0° and 90° directions. In this plot the higher order reflections are more evident. There is virtually no scattering in a sector oriented along the 0° direction showing that cylinders are strongly oriented along the shear direction. A better estimate of the degree of orientation can be obtained by plotting the integrated intensity of (10) reflection vs azimuthal angle ($I_{10}(\phi)$ vs $\phi$), as shown in Figure 10C. The presence of two intense and narrow peaks at −90° and +90° with (hwhm) only 5° indicates that cylinder axes are oriented almost perfectly along the shear direction.

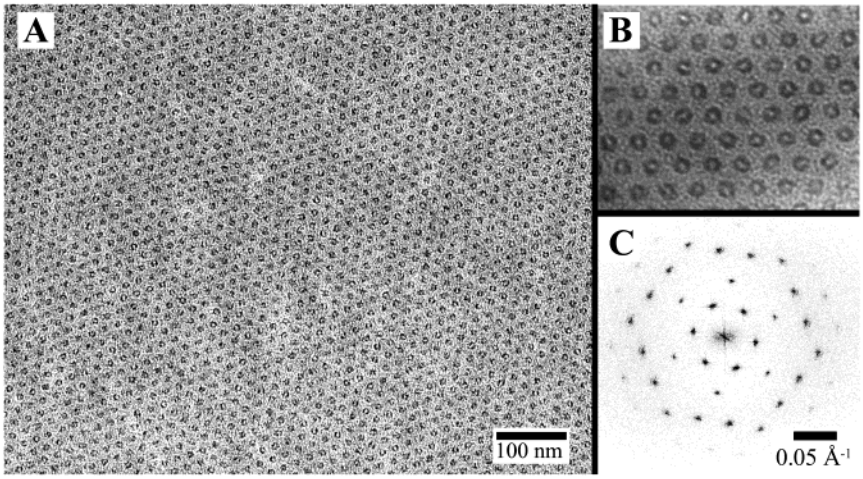


**Figure 12.** (A) Transmission electron micrograph of the shear aligned CEC50 sample. Ultrathin section is microtomed perpendicular to the shear direction, and the TEM image shows a long-range hexagonal arrangement of the PE cylinders. $RuO_4$ staining is used to enhance the contrast between the semicrystalline PE and the amorphous PCHE. (B) Higher magnification TEM image showing light gray PCHE matrix, almost black amorphous PE cylinder shell and white crystalline PE cylinder core. (C) The FFT spectrum of a 1.5 $\mu$m × 1.5 $\mu$m TEM image.

To investigate how cylinders are packed at the microscopic level, a TEM study was performed. $RuO_4$ solution staining was used in order to enhance contrast between PE and PCHE domains. $RuO_4$ staining for these materials relies on the different rates of diffusion of the stain in amorphous PCHE, amorphous PE, and crystalline PE.

The TEM image shows that cylinders are ordered along the shear direction and packed in a hexagonal lattice (Figure 12A). The higher magnification inset in the upper corner indicates that there are three levels of contrast present in these images. Inside the cylinders is a nearly white cylinder core, which contains high-density PE crystallites. The amorphous PE near the block copolymer interface at the cylinder shell regions is stained most and it is almost black, and the amorphous PCHE matrix is gray. The inset in the lower right corner shows the FFT of the TEM image shown in Figure 12A, but from a slightly larger area (approximately 1.5 $\mu$m × 1.5 $\mu$m). The FFT shows a very strong hexagonal spot pattern for (10), (11), (21), and (30) reflections, and some faint higher order reflections are also present. It is evident from the FFT and the TEM images that the grains extend over the size of TEM images (> microns), and only a few dislocations are present in each image. Note that the (20) reflection is missing in the FFT spectrum taken from the TEM image, which can be interpreted to be a result of the minimum in the form factor for this particular cylindrical structure. However, in SAXS diffraction patterns a strong (20) peak was always observed, which indicates that lattice constants may have changed considerably when preparing samples for TEM. Indeed, the long period determined from the TEM image was surprisingly small. Even after recalibrating the TEM magnifications using monodisperse PS latex particles and a carbon grating grid, the long period (i.e., (10) lattice planes) was 16.4 nm. The corresponding long period from SAXS measurement was 21.6 nm. This extensive $RuO_4$ staining seems to have a large effect on the cylinder spacing in the sample. The sample surface was also observed to crack during staining due to strong shrinkage stresses. In this paper $RuO_4$ staining was used only to study domain orientation in TEM, and all the fracture experiments were performed using thicker, unstained films.

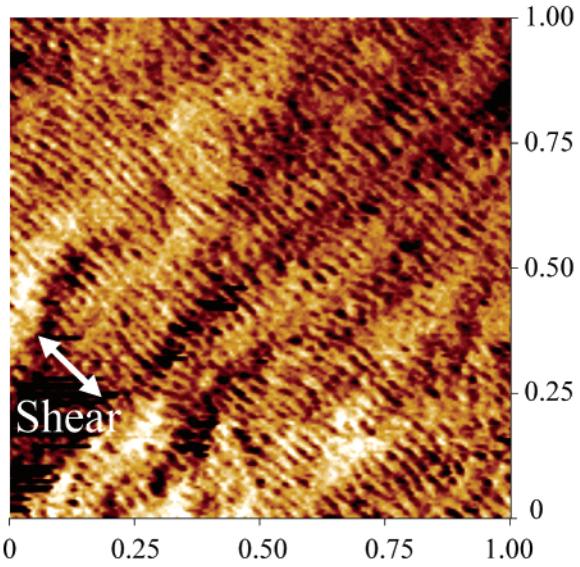


**Figure 13.** SFM phase image of the microtomed CEC50 film, 1 $\mu$m scan. The SFM scan was done on actual 1 $\mu$m thick free-standing film mounted on the copper grid.

To investigate fracture properties of the shear aligned samples, 1 $\mu$m thick sections were cut using an ultramicrotome and diamond knife. The sample orientation was selected so that cylinders were always parallel with respect to the film surface and either parallel or perpendicular to the strain axis. The SFM image in Figure 13 shows the surface morphology of the sample after microtoming. Cylinders are clearly lying parallel with respect to the film surface, and their orientation is along the shear axis. The SFM scan was done on an actual 1 $\mu$m film mounted on the copper grid before the fragility test was carried out.

In these fragility tests the cylinder orientation was either perpendicular or parallel to the strain direction. The median strain for crazing is 0.5% for both orientations, which is very close to the values obtained without shear orientation for the spun-cast samples. The cumulative fraction of film squares that has failed due to

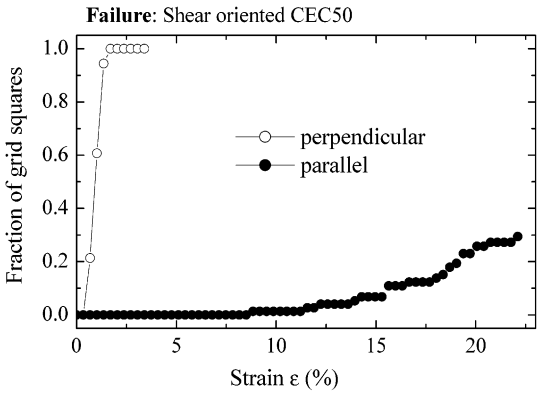


**Figure 14.** Cumulative number fraction of shear aligned CEC50 film squares that have failed as a function of strain. Microtomed 1 $\mu$m thick films were mounted onto the copper grids so that the PE cylinders were oriented either perpendicular (open circles) or parallel (solid circles) to the applied strain.

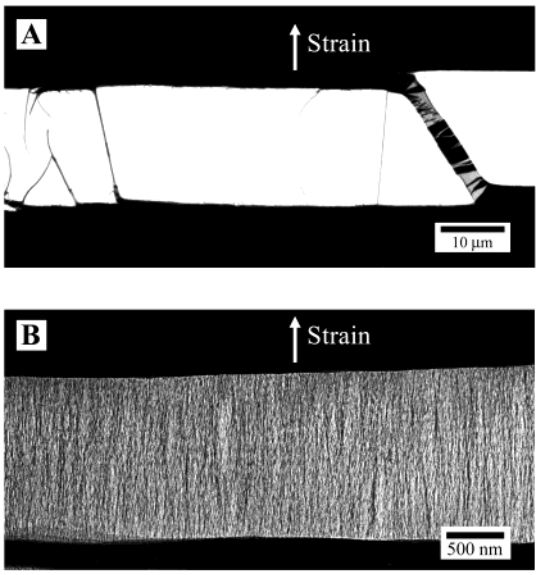


**Figure 15.** (A) Transmission electron micrographs of the shear-aligned CEC50 samples after the fragility test. (a) PE cylinders are oriented perpendicular to the strain. Applied strain is 1%, and the crack has already propagated through the 1 mm wide film square. (B) When the PE cylinders are aligned parallel to the strain, stable craze matter can grow. TEM image is taken at 20% strain.

crack propagation is shown in Figure 14. Perpendicularly oriented polyethylene cylinders cannot hold the load, and film failure follows soon after crazing. The median strain for failure is 0.9%, which is also roughly the same as for spun-cast films. Note that, for this low molecular weight CEC50, the PE cylinders in spun-cast films were ordered predominantly normal to film surface and thus perpendicular to the applied strain already after spin-casting.

Figure 15A shows a TEM micrograph of a film square strained in tension perpendicular to the PE cylinders. The TEM image is taken at the strain level where the crack has just propagated through the 1 mm wide sample, and the film is still held together with the small domains where the PE cylinders are oriented perpendicular to the crack. These small bridges are formed during the crack propagation due to the slight cylinder misalignment with respect to the strain. Inside of these small domains the PE cylinders are reoriented parallel to the strain, and therefore they can hold a significant amount of load. But despite the fact that these small domains can stretch plastically significantly without breaking, macroscopically the sample fails at low overall strains due to very small size of these domains.

The mechanical properties are quite different if the PE cylinder axes are oriented parallel to the strain direction. Although the median value for the crazing strain is again roughly the same as that for the spun-cast samples, there is no significant failure up to 15% strain, and approximately 30% of the grid squares have failed at 22% strain (Figure 14). Crazes propagate quickly across the 1 mm wide film squares and start to grow in lateral width. Figure 15B shows a TEM image of typical crazes taken at 20% strain. The craze width is about 1.5 $\mu$m, and the strain direction is perpendicular to crazes. Because PE cylinders are oriented across the craze, very stable craze growth can occur. The deformation and the failure mechanism are same for parallel or perpendicular cylinder orientations: crazing and failure due to crack propagation. Although craze initiation is not affected by domain orientation, the craze breakdown and crack propagation are strongly hindered if the PE cylinders are aligned parallel to strain.

**Deformation Mechanisms.** The main deformation mechanism for all block copolymers studied in this paper is plastic deformation by crazing. The higher molecular weight samples also showed mixed deformation by crazing and shear yielding if they were not physically aged. Although we do not have any direct proof, we have strong circumstantial evidence that in the CEC system craze initiation and growth proceeds by cavitation and voiding in the continuous PCHE matrix rather than in the semicrystalline PE domains. Increased craze stability and resistance to large strains is achieved by incorporation of fibrillated PE into the craze. In the case of physically aged samples an increased strain to failure of the CEC polymer films was only observed when PE cylinders formed continuous structures along the tensile strain direction, i.e., either a random network of PE cylinders or PE cylinders oriented parallel to the tensile strain. In the CEC system PE cylinders are not connected to each other by PCHE bridging chains, and therefore when the PE cylinders are oriented transverse to the strain direction, incorporation of PE into the craze fibril structure is hindered. More support for this idea can be obtained by studying the pentablock polymer CECEC where all cylinders are connected by bridging PCHE middle block chains. Pentablock polymers are ductile regardless of the cylinder orientation and sample thermal history.[16]

Early studies have already shown that chain architecture is important for determining the block copolymer toughness. Matsuo et al. studied PS−PB block copolymers where the PB block forms cylinders in a PS matrix.[8] They observed that diblock (SB) and triblock copolymers (BSB) where PB is the end block are brittle. In contrast, similar molecular weight triblock copolymers where butadiene was the middle block (SBS) and tetrablock copolymers (SBSB) were tough and resisted fracture to large strains. These finding are consistent with studies showing that diblock copolymers (CE) and triblock copolymers (ECE) are brittle.[32] The triblock copolymers with a PE middle block (CEC) are either ductile or brittle depending on the cylinder orientation and thermal history whereas a relatively low molecular weight pentablock copolymer (CECEC with $M_w = 60\,000$ g/mol and $f_{PE} = 0.25$) is ductile under all conditions.

The deformation mechanism for SB diblock copolymers having a glassy PS matrix is first by cavitation of rubbery PB domains followed by PS fibril drawing and craze formation.[33] The same mechanism is also observed for PS−PBMA diblock copolymer systems and PBMA−PS−PBMA triblock copolymers, where the end blocks are "softer" and the middle PS block forms the matrix.[9,10] On the other hand, for (SBS) systems where end blocks form a glassy matrix, cavitation or voiding is observed in the PS domains. Voiding in the continuous PS matrix rather than in the rubber domains was attributed to the high concentration of chain ends in the PS matrix.[34] By analogy with SBS, in CEC block copolymers the unentangled end blocks form the continuous glassy matrix, so voiding in the PCHE matrix rather than in the highly entangled PE domains may be expected.

## Summary

In the present study the deformation and fracture properties of films of semicrystalline−glassy CEC triblock copolymers were investigated. This work was limited to block copolymer compositions where semicrystalline PE domains form cylinders in a glassy PCHE matrix. The deformation was observed to be strongly dependent on amount of physical aging in PCHE domains and on the PE cylindrical microdomain orientation. When the cylinder orientation was "random" or parallel to applied strain, ductile behavior was observed irrespective of the sample thermal history. When PE cylinder axes were oriented normal to the film and therefore transverse to the applied strain, very brittle behavior was observed for physically aged samples. If the effects of physical aging are removed by quenching from the melt, CEC films show ductile behavior even when the cylinders are oriented perpendicular to the principal axis of tensile strain.

**Acknowledgment.** This work was supported by the Material Research Laboratory program of the National Science Foundation under Award DMR00-80034 and by a gift from the Dow Chemical Co.

## References and Notes

(1) Yang, A. C.-M.; Kramer, E. J.; Kuo, C. C.; Phoenix, S. L. *Macromolecules* **1986**, *19*, 2010.
(2) Bates, F. S.; Fredrickson, G. H.; Hucul, D.; Hahn, S. F. *AIChE J.* **2001**, *47*, 762.
(3) Seymour, R. B. *Adv. Chem. Ser.* **1989**, *222*, 3.
(4) Khanarian, G. *Polym. Eng. Sci.* **2000**, *40*, 2590.
(5) Echte, A. *Adv. Chem. Ser.* **1989**, *222*, 15.
(6) Bates, F. S.; Fredrickson, G. H. *Annu. Rev. Phys. Chem.* **1990**, *41*, 525.
(7) Hamley, I. W. *The Physics of Block Copolymers*; Oxford University Press: New York, 1998.
(8) Matsuo, M.; Ueno, T.; Horino, H.; Chujyo, S.; Asai, H. *Polymer* **1968**, *9*, 425.
(9) Weidisch, R.; Ensslen, M.; Michler, G. H.; Fischer, H. *Macromolecules* **1999**, *32*, 5375.
(10) Weidisch, R.; Ensslen, M.; Michler, G. H.; Arnold, M.; Budde, H.; Höring, S.; Fischer, H. *Macromolecules* **2001**, *34*, 2528.
(11) Struik, L. C. E. *Physical Aging in Amorphous Polymers and Other Materials*; Elsevier: Amsterdam, 1978.
(12) Donald, A. M.; Kramer, E. J. *J. Mater. Sci.* **1982**, *17*, 1871.
(13) Keller, A.; Pedemonte, E.; Willmouth, F. M. *Nature (London)* **1970**, *225*, 538.
(14) Keller, A.; Pedemonte, E.; Willmouth, F. M. *Kolloid Z. Z. Polym.* **1970**, *238*, 385.
(15) Schwier, C. E.; Argon, A. S.; Cohen, R. E. *Polymer* **1985**, *26*, 1985.
(16) Ryu, C. Y.; Ruokolainen, J.; Fredrickson, G. H.; Kramer, E. J.; Hahn, S. F. *Macromolecules* **2002**, *35*, 2157.
(17) Weimann, P. A.; Hajduk, D. A.; Chu, C.; Chaffin, K. A.; Brodil, J. C.; Bates, F. S. *J. Polym. Sci., Part B: Polym. Phys.* **1999**, *37*, 2053.
(18) Kramer, E. J.; Berger, L. L. *Adv. Polym. Sci.* **1990**, *91/92*, 1.
(19) Brown, G. M.; Butler, J. H. *Polymer* **1997**, *38*, 3937.
(20) Vigild, M. E.; Chu, C.; Sugiyama, M.; Chaffin, K. A.; Bates, F. S. *Macromolecules* **2001**, *34*, 951.
(21) Huang, E.; Russell, T. P.; Harrison, C.; Chaikin, P. M.; Register, R. A.; Hawker, C. J.; Mays, J. *Macromolecules* **1998**, *31*, 7641.
(22) Mansky, P.; Russell, T. P.; Hawker, C. J.; Pitsikalis, M.; Mays, J. *Macromolecules* **1997**, *30*, 6810.
(23) Brown, H. R.; Kramer, E. J. *J. Macromol. Sci., Phys.* **1981**, *B19*, 487.
(24) Yang, A. C. M.; Kramer, E. J. *J. Polym. Sci., Part B: Polym. Phys.* **1985**, *23*, 1353.
(25) Brown, H. R. *Ultramicroscopy* **1982**, *7*, 263.
(26) Ductile means here that sample does not fail before the copper grid fails at the strain approximately 25%.
(27) Rangarajan, P.; Register, R. A.; Fetters, L. J. *Macromolecules* **1993**, *26*, 4640.
(28) Brandrup, J.; Immergut, E. H.; Grulke, E. A. *Polymer Handbook*, 4th ed.; Wiley: New York, 1999.
(29) Hasan, O. A.; Boyce, M. C. *Polymer* **1993**, *34*, 5085.
(30) Henkee, C. S.; Kramer, E. J. *J. Polym. Sci., Polym. Phys. Ed.* **1984**, *22*, 721.
(31) Hamley, I. W. *J. Phys: Condens. Matter* **2001**, *13*, R643.
(32) Bates, F. S. Private communication.
(33) Argon, A. S.; Cohen, R. E.; Gebizlioglu, O. S.; Schwier, C. E. *Adv. Polym. Sci.* **1983**, *52/53*, 275.
(34) Koltisko, B.; Hiltner, A.; Baer, E.; Tung, L. H. *J. Polym. Sci., Part B: Polym. Phys.* **1986**, *24*, 2167.

MA020791K